Biomechanics and Modeling in Mechanobiology (2024) 23:1197–1207
https://doi.org/10.1007/s10237-024-01833-7

ORIGINAL PAPER

Frequency and time dependent viscoelastic characterization of pediatric porcine brain tissue in compression

Weiqi Li[1] · Duncan E. T. Shepherd[2] · Daniel M. Espino[2]

Received: 17 November 2023 / Accepted: 20 February 2024 / Published online: 14 March 2024

Abstract
Understanding the viscoelastic behavior of pediatric brain tissue is critical to interpret how external mechanical forces affect head injury in children. However, knowledge of the viscoelastic properties of pediatric brain tissue is limited, and this reduces the biofidelity of developed numeric simulations of the pediatric head in analysis of brain injury. Thus, it is essential to characterize the viscoelastic behavior of pediatric brain tissue in various loading conditions and to identify constitutive models. In this study, the pediatric porcine brain tissue was investigated in compression with determine the viscoelasticity under small and large strain, respectively. A range of frequencies between 0.1 and 40 Hz was applied to determine frequency-dependent viscoelastic behavior via dynamic mechanical analysis, while brain samples were divided into three strain rate groups of 0.01/s, 1/s and 10/s for compression up to 0.3 strain level and stress relaxation to obtain time-dependent viscoelastic properties. At frequencies above 20 Hz, the storage modulus did not increase, while the loss modulus increased continuously. With strain rate increasing from 0.01/s to 10/s, the mean stress at 0.1, 0.2 and 0.3 strain increased to approximate 6.8, 5.6 and 4.4 times, respectively. The brain compressive response was sensitive to strain rate and frequency. The characterization of brain tissue will be valuable for development of head protection systems and prediction of brain injury.

Keywords Brain · Constitutive · Dynamic mechanical analysis · Injury · Porcine · Viscoelastic

1 Introduction

Brain tissue can be damaged given external mechanical force even though it is surrounded by the skull. Traffic accidents, abuse and falls are primary causes of traumatic brain injury (TBI) in children (Araki et al. 2017; Hon et al. 2019). Mild traumatic brain injury (mTBI), such as concussion, is one of the most common types of TBI for the overall population (Nguyen et al. 2016) and damage caused by direct concussive loading can occur both in the region of impact and in regions distant from the impact site (Meaney and Smith 2011). The symptoms of brain injuries including loss of consciousness, headaches and mood changes can appear immediately or several weeks later (Pujalte et al. 2020). Due to the development of computational modelling and medical imaging techniques, head simulation models have been applied intensively to study injury mechanisms and predict biomechanical characterization of brain injury induced by different impact conditions (Roth et al. 2010; Sahoo et al. 2014). Besides the accurate anatomical structures, the biofidelity of the finite element (FE) simulation models requires quantitative data from mechanical experiments to accurately relate tissue stress to tissue deformation and is highly dependent on the constitutive models applied.

Over the past decades, many experiments have been performed to investigate the mechanical properties of brain tissue obtained from adult human and animal brains (Bilston et al. 2001; Budday et al. 2015; Rashid et al. 2012; Takhounts et al. 2003). However, the mechanical analysis of brain tissue obtained from pediatric cadavers has been limited. Some studies investigated brain tissue through dynamic sweep tests in the frequency domain, while stress relaxation tests in the time domain have also been carried out (Darvish and Crandall 2001; Velardi et al. 2006). Furthermore, indentation tests, considered as a type of compression, were also employed to characterize the viscoelastic properties of brain

✉ Weiqi Li
liweiqi1010@163.com

[1] School of Health Science and Engineering, University of Shanghai for Science and Technology, Shanghai 200093, China

[2] Department of Mechanical Engineering, University of Birmingham, Birmingham B15 2TT, UK

tissue (Chen et al. 2020; Feng et al. 2013; Qiu et al. 2020). Child brain samples, between the age of 5 months and 22 months, have been previously studied through dynamic oscillatory shear experiments showing age-dependent material properties (Chatelin et al. 2012). In addition, shear relaxation tests on the brain of a 5-year-old child were conducted to analyze the shear stresses under large deformation conditions (Prange 2002). Most experiments were performed in shear, while compressive loading also plays a significant role during head injuries (Bar-Kochba et al. 2016; Young et al. 2015). Thus it is essential to understand the compressive behavior of pediatric brain tissue in both time and frequency domains. Considering the similarities of the anatomical structure between human and animal brains, young animal brain tissue including immature porcine and mouse brains has also been selected as a substitute for children in previous studies to determine the brain's mechanical properties (Li et al. 2019; MacManus et al. 2017; Prange and Margulies 2002; Zhao et al. 2016).

To investigate the relationship between the mechanical characteristics of human and animal brain, various mechanical experiments have been performed (Dickerson et al. 1967; Franklyn et al. 2007). Compression tests were conducted on porcine brain tissue for three age groups at different strain rates (Fan et al. 2014). Shear tests were carried out on brain tissue derived from 5-day-old, 4-week-old piglets and 1-year-old pigs (Prange and Margulies 2002). Large strain and various strain rates were applied on 8-week-old pig brain tissue through compression to investigate the material properties (Li et al. 2019). Tension tests with dynamic strain rates were performed on the cerebellum and the brainstem tissue of piglets aged 4 weeks to determine the strain-dependent properties (Zhao et al. 2016). Further, the mechanical behavior of 8-week-old porcine brain tissue has been investigated through the combination of compression, shear and tensile tests to analyze the region and strain-rate dependent properties (Li et al. 2020a, b). For brain tissue experiencing small deformation, linear viscoelastic models were commonly used for modelling (Qian et al. 2018) while in large strain conditions, quasi-linear viscoelastic models composed of a hyperelastic part and a linear viscoelastic part were used (Rashid et al. 2014).

The aim of this study was to characterize the viscoelastic properties of pediatric porcine brain tissue in compression through Dynamic Mechanical Analysis (DMA) over a frequency range which is relevant to physiology and trauma, and under nonlinear deformation over three strain rates. The effect of frequency and strain rate on the viscoelastic behavior of brain tissue have been evaluated statistically. Linear and non-linear viscoelastic models have been assessed by employing the experimental data to determine material parameters appropriate for the computational modelling of brain tissue. This work was organized as follows: Sect. 2 presented the methodology to carry out the experiments on the brain tissue and the constitutive formulation with linear and large strain viscoelastic models. The experimental results with corresponding constitutive models were displayed in Sect. 3. Section 4 discussed the effects of loading conditions on the mechanical responses of the brain tissue. Finally, the main conclusions obtained were given in Sect. 5.

2 Materials and methods

2.1 Specimen preparation

Seven porcine brains of approximately 4 months age were obtained from a supplier (Dissect Supplies, Kings Heath, Birmingham, UK). Specimens were wrapped in tissue paper, and soaked in Ringer's solution (Oxoid Ltd, Basingstoke, UK), on arrival in the laboratory. Specimens were then stored at −40 °C in a freezer in double heat-sealed plastic bags (Burton et al. 2017; Mahmood et al. 2018). Specimens were thawed in Ringer's solution for 12 h before mechanical testing. The freezing treatment has not been found to adversely affect the mechanical properties of biological tissue (Chan and Titze 2003; Szarko et al. 2010). The cerebellum and brain stem were removed, and cylindrical specimens which comprised both white and grey matter were obtained from the frontal, parietal and occipital lobes of cerebrum in the coronal plane using a circular trephine. Brain samples were 7 ± 1 mm (mean ± standard deviation) in thickness and 28 ± 0.1 mm in diameter, measured prior to testing using a Vernier calliper (Draper Tools Ltd, Hampshire, UK).

2.2 Experimental setup

The mechanical properties of brain specimens were determined using a Bose ElectroForce 3200 (Bose Corporation, ElectroForce Systems Group, Minnesota, USA) testing machine as shown in Fig. 1a. The apparatus was equipped with a 22 N load cell and a linear displacement transducer with a range of 8 mm displacement. A custom-designed chamber with a 28 mm diameter was used to hold and constrain the brain specimens. To minimize the influence of friction during compression, specimens and the surface inside the chamber were hydrated with Ringer's solution before each test. A circular flat indenter with a diameter of 20 mm, attached to the actuator of the testing machine, was used to generate compressive forces (Fig. 1b). After the load and displacement values were set to zero, a preload of −10 mN was applied to the brain samples to ensure a zero-strain. The negative sign in the stress and strain denotes the compression of brain tissue. All samples were tested at room

Fig. 1 (**a**) Experimental set-up of a Bose ElectroForce 3200 testing system with WinTest software and (**b**) compressive testing setup for the brain specimens

temperature (21 °C) and fully hydrated in Ringer's solution throughout preparation and testing.

2.3 Dynamic mechanical analysis (DMA)

DMA testing was used to measure the viscoelastic properties of the brain tissue over a frequency range from 0.1 to 40 Hz in 13 steps. The testing frequencies cover the loading conditions to which the brain might be exposed during physiological and mild traumatic loading (Laksari et al. 2015; Yan et al. 2015). Amplitude sweep tests at 1 Hz were performed to determine the amplitude range within the linear viscoelastic regime of the material and a 1% dynamic amplitude was selected in the subsequent dynamic testing. Parameters of testing and specimen geometry were inputted into the WinTest DMA software, which provides improved test control and analysis for viscoelastic property measurement of materials in DMA. All DMA tests were performed with the sampling rate of acquisition at 5 kHz for the highest frequency tested. An example of the raw data of stress against strain was shown in Fig. 2. Prior to the frequency sweep testing, brain specimens were subjected to an initial ramp of 10% pre-strain to ensure robust sample contact and a preconditioning cycle of 5 Hz with 0.07 mm amplitude to minimize the sample variability (Cheng et al. 2009; Li et al. 2020a, b; Wilcox et al. 2014). Twelve specimens were tested using this protocol across a range of frequencies tested. The storage modulus is the elastic component of the dynamic modulus relating to the spring constant, and the loss modulus is the viscous component of modulus relating to damping. The ratio of loss to storage modulus ($G^{''}/G^{'}$) is defined as tan(delta), which is a measure of energy dissipation in a system. For each frequency, sinusoidal force and displacement data were recorded and subjected to analysis using Fast Fourier Transform (FFT) methodology. The dynamic stiffness (k^*) was calculated as the ratio of the data-set magnitude for force and displacement at the fundamental frequency. Storage

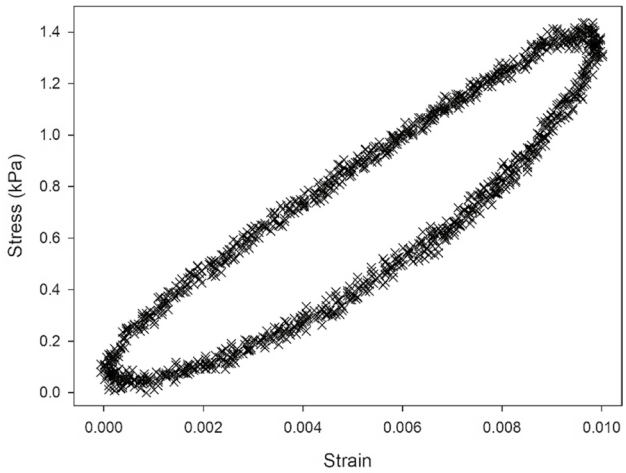

Fig. 2 Representative stress strain experimental data, from multiple cycles, for a given sample at 40 Hz

modulus ($G^{'}$) and loss modulus ($G^{''}$) were subsequently quantified in WinTest DMA software by transforming from the relevant stiffness, incorporating a shape factor (S) for cylindrical samples:

$$G' = \frac{k^* \cos\delta}{S} \tag{1}$$

$$G'' = \frac{k^* sin\delta}{S} \tag{2}$$

$$S = \frac{\pi d^2}{4h} \tag{3}$$

where h and d denote the thickness and diameter of the specimen, respectively. The phase angle (δ) was determined as the phase relationship between the compressive force and displacement. Further details are available elsewhere (Barnes et al. 2016).

2.4 Compression-relaxation tests

To investigate the compressive viscoelastic properties of brain tissue at large strain, the specimens were compressed by the indenter up to the displacement of 30% of the height of the specimens (i.e. 0.3 nominal strain). The tests were conducted at three pre-set deformation velocities of 0.07 mm/s (low), 7 mm/s (medium) and 70 mm/s (high), corresponding to the strain rates of 0.01/s, 1/s and 10/s, respectively. The force–displacement history was recorded with a sampling rate of 1 kHz. These testing velocities were comparable to the range of the frequencies applied in Sect. 2.3 and with previous studies on human and porcine brains (Forte et al. 2017; Li et al. 2019). Five specimens were tested at each velocity. Totally, 27 brain specimens from seven porcine brains were tested including 12 specimens for DMA tests and 15 specimens for compression-relaxation tests. After the compression of 0.3 strain, the stress-relaxation behavior of pediatric brain was observed by holding the peak strain for 200 s describing the viscous response of the material. Before compression-relaxation testing, specimens were subjected to two pre-conditioning cycles with 10% strain to ensure comparable and repeatable results, consistent to previous studies on brain tissue (Budday et al. 2017a, b; Prange and Margulies 2002). The engineering stress was calculated as the applied force divided by the nominal cross-sectional area which was a certain value given the size of the circular indenter, and the engineering strain was calculated as the deformation divided by the initial height of sample measured prior to mechanical testing.

Experimental values were analyzed and plotted using Sigmaplot version 14.5 (Systat Software Inc., London, UK), and the effect of strain rates on stress for compression tests was determined using a one-way analysis of variance (ANOVA) test, by comparing the mean stress levels induced at fixed strain increments (0.1, 0.2 and 0.3) between strain rate groups with a Tukey HSD post-hoc analysis. For each strain rate group, stress levels not sharing a letter are considered significantly different. Statistical significance was evaluated at the $p < 0.05$ level.

2.5 Viscoelastic formulation

2.5.1 Linear viscoelastic model

Linear viscoelastic (LV) theory was previously applied to represent the mechanical response of brain injury in the time domain (Qian et al. 2018). In this study, the specimens were tested using DMA within the linear viscoelastic regime. To describe the dynamic frequency-dependent viscoelastic properties of brain tissue, the constitutive parameters can be obtained directly from frequency domain experimental data.

The complex modulus $G^* = G\prime + jG''$, the storage modulus $G\prime$ and the loss modulus G'' of the generalized Maxwell model in the Prony series form can be obtained as functions of frequency:

$$G^*(j\omega) = G_e + \sum_{i=1}^{N} g_i \frac{\tau_i j\omega}{1 + \tau_i j\omega} \tag{4}$$

$$G'(\omega) = G_e + \sum_{i=1}^{N} g_i \frac{(\omega\tau_i)^2}{1 + (\omega\tau_i)^2} \tag{5}$$

$$G''(\omega) = \sum_{i=1}^{N} g_i \frac{\omega\tau_i}{1 + (\omega\tau_i)^2} \tag{6}$$

where ω is a single angular frequency, G_e is the equilibrium modulus and $j = \sqrt{-1}$ standing for the imaginary number. In the linear viscoelastic model, parameters g_i and τ_i are the relative moduli and the relaxation time of the Prony series for N relaxation modes. Further details on the frequency domain modelling are available elsewhere (Li et al. 2021a). The constitutive parameters were calibrated using a nonlinear least-squares algorithm lsqnonlin in MATLAB with the average experimental data of tested tissue samples based on the average square of deviation between the predicted dynamic modulus $(G'(\omega_i), G''(\omega_i))$ and the measured dynamic modulus $(\overline{G}_i', \overline{G}_i'')$ from experiment at n frequencies ω_i:

$$\min\left\{\sum_{i=1}^{n}\left(\left(\frac{G'(\omega_i)}{\overline{G}_i'} - 1\right)^2 + \left(\frac{G''(\omega_i)}{\overline{G}_i''} - 1\right)^2\right)\right\} \tag{7}$$

2.5.2 Large strain viscoelastic model

Within non-linear viscoelasticity, quasi-linear viscoelastic (QLV) theory has been assumed for soft biological tissue experiencing nonlinear strain conditions (Mendizabal et al. 2015), and it assumes the material behavior to be decoupled into two responses including a time-independent elastic response and a viscoelastic response. For the elastic response, a hyperelastic material model was used to describe the compressive properties of brain tissue for large strain analysis and the brain was considered as an isotropic incompressible material characterized by a strain-energy function W, such that.

$$S_{11} = \frac{dW}{d\lambda} \tag{8}$$

$$W = W\left(I_1, I_2\right) or W = W(\lambda_1, \lambda_2, \lambda_3) \tag{9}$$

where S_{11} is the nominal stress component along the direction of compression. I_1 and I_2 are the first and second strain invariants. λ_1, λ_2, λ_3 are the principal stretches. Three established hyperelastic constitutive models were evaluated (Table 1) and model parameters were determined using nonlinear optimization in MATLAB with the randomly generated starting parameter set to achieve the global optimal set. The appropriateness of fit of data to the given model was assessed using the coefficient of determination R^2 for various loading rates.

For the viscoelastic responses, the large strain viscoelastic model was described by a Prony series expansion of the relaxation modulus combined with the strain energy function from Table 1 to describe the time-dependent properties (Miller and Chinzei 1997),

$$\varphi(t) = \int_0^t \left\{ g_d(t-\tau)\frac{dw}{d\tau} \right\} d\tau \tag{10}$$

where φ is time dependent strain energy, $w = W/\mu_0$ is a dimensionless strain-energy function. The viscoelastic behavior was therefore presented by the time-dependent shear modulus (Rashid et al. 2012),

$$g_d(t) = \mu_0 \left[1 - \sum_{p=1}^{N} g_p \left(1 - e^{-\frac{t}{\tau_p}} \right) \right] \tag{11}$$

where μ_0 is the initial shear modulus and can be obtained from the time-independent large strain response of the tissue. g_p and τ_p are material parameters of the pth term in the number N Prony series and determined by fitting $g_d(t)$ with experimental values obtained from the relaxation tests. A minimum of three pairs of Prony constants was deemed necessary for replicating the time-dependent behavior of brain tissue (Cheng and Bilston 2007; Forte et al. 2017) and the preliminary studies indicated that a three-term Prony series was needed for the brain viscoelastic response.

3 Results

3.1 Linear viscoelasticity

The mean storage modulus of brain samples showed an increasing trend initially with frequency and then decreased at higher frequencies with an average value of 10.94 kPa (Fig. 3a). The mean loss modulus of brain samples showed an increasing trend for all frequencies tested ranging from 1.61 to 11.38 kPa with an average value of 6.68 kPa (Fig. 3b). Notably, at frequencies above 20 Hz, storage modulus did not increase, while the loss modulus increased continuously. This was also reflected by the linear viscoelastic constitutive model calibrating the mean storage and loss modulus simultaneously with all viscoelastic response approximated within the 95% confidence intervals (Fig. 3a and b). The model was able to predict the increasing trend of storage modulus up to around 20 Hz and loss modulus of all frequencies tested. Table 2 summarizes the material parameters of the linear viscoelastic model with the equilibrium modulus of 268.46 Pa and the quality of the calibration was tested by evaluating the coefficient of determination with $R^2 = 0.85$ for storage modulus and $R^2 = 0.94$ for loss modulus. The comparatively low coefficient of determination in storage modulus arises from the decreasing trend at frequencies above 20 Hz which might be due to the lateral confinement of the specimens in compressive frequency sweep testing.

The mean complex modulus of brain tissue with an average value of 13.02 kPa increased rapidly at frequencies between 0.1 and 20 Hz (Fig. 3c). The mean tan(delta) of brain samples showed an increasing trend with frequency, ranging from 0.28 to 1.08, with higher values beyond 20 Hz, signifying a more dominant viscous response occurring (Fig. 3d).

3.2 Large strain viscoelasticity

With the strain rate increasing from 0.01/s to 10/s, the mean stress at 10, 20 and 30% strain increased to approximate 6.8, 5.6 and 4.4 times, respectively (Fig. 4a). For all three

Table 1 Incompressible strain energy functions and the uniaxial stress expression for each hyperelastic model

Hyperelastic model	Strain energy function	Uniaxial stress expression
Neo-Hookean	$W = \frac{\mu_0}{2}(I_1 - 3)$	$S_{11} = \mu_0(\lambda - \lambda^{-2})$
Gent	$W = -\frac{\mu_0}{2} J_m \ln\left(1 - \frac{I_1 - 3}{J_m}\right)$	$S_{11} = \frac{\mu_0 J_m}{J_m - \lambda^2 - 2\lambda^{-1} + 3}\left(\lambda - \lambda^{-2}\right)$
Ogden	$W = \frac{2\mu_0}{\alpha^2}\left(\lambda_1^{\alpha} + \lambda_2^{\alpha} + \lambda_3^{\alpha} - 3\right)$	$S_{11} = \frac{2\mu_0}{\alpha}\left\{\lambda^{\alpha-1} - \lambda^{-\left(\frac{\alpha}{2}+1\right)}\right\}$

Coefficients μ_0, J_m and α are the material parameters and λ is the principle stretch in the uniaxial loading direction

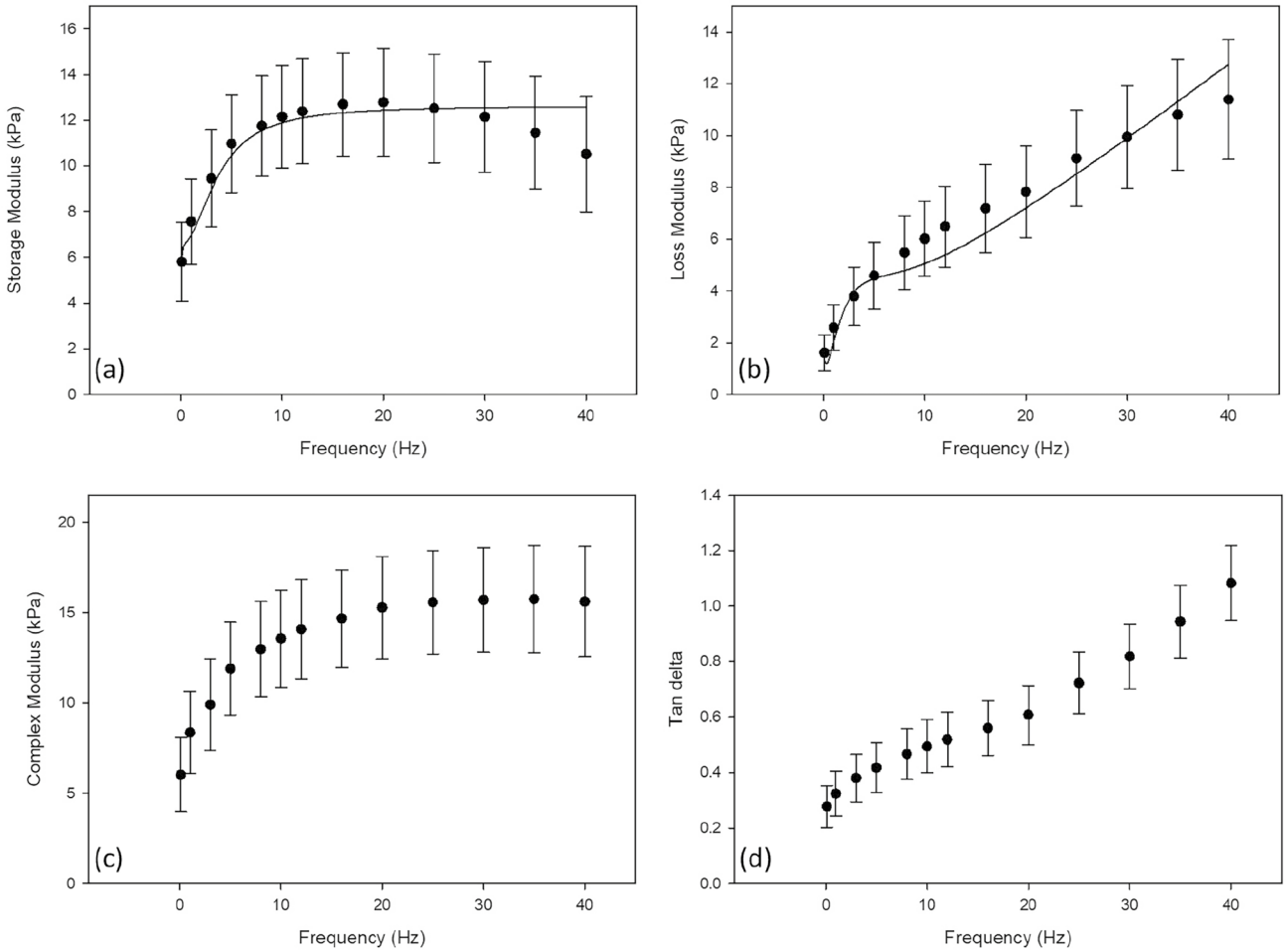

Fig. 3 Variation of (**a**) mean storage modulus, (**b**) mean loss modulus, (**c**) mean complex modulus and (**d**) tan(delta) for all brain samples against frequency using DMA, with the relevant linear viscoelastic model (full black line) calibrated from the experimental storage and loss modulus for all frequencies tested. Error bars represent 95% confidence intervals

Table 2 Constitutive parameters of frequency-dependent linear viscoelastic model derived from mean storage and loss modulus of brain tissue simultaneously over all frequencies

Linear viscoelastic model parameter					
Coefficient (kPa)			Relaxation time (s)		
g_1	g_2	g_3	τ_1	τ_2	τ_3
3.1×10^{4}	5.9×10^{1}	5.5×10^{1}	1.5×10^{-6}	4.6×10^{-2}	7.5×10^{3}

strain increments, the stress at the high strain rate was significantly different from that of the medium and low strain rates ($p<0.05$), and the stress levels at the medium and low strain rate groups were not significantly different from each other (Fig. 4b). Mean compressive stress–strain responses displayed an increase in the stiffness of the material with strain up to around −0.2, and at higher strain level, the stiffness then decreased to be stable, especially at higher strain rate which might be due to some experimental artifacts including the possible smoothed displacement profile of the indenter.

Three hyperelastic constitutive models were compared to assess their performance in representing the hyperelastic behavior of brain tissue using the time-independent elastic experimental data of stress–strain response at different strain rate groups (Fig. 5). The corresponding material parameters and coefficients of determination of three strain rate groups are summarized in Table 3. As the compressive behavior of brain deviated from linearity, the Neo-Hookean constitutive model was not able to predict the experimental data. While the Ogden and Neo-Hookean constitutive models represented the mechanical behavior, when calibrated with each strain rate, the experimental data deviated from model predictions as the strain was close to 0.3. This may indicate that the calibration of the models overestimated the actual experimental results for this strain level.

The mean stress curves across a range of strain rates are shown in Fig. 6. The material relaxation showed an

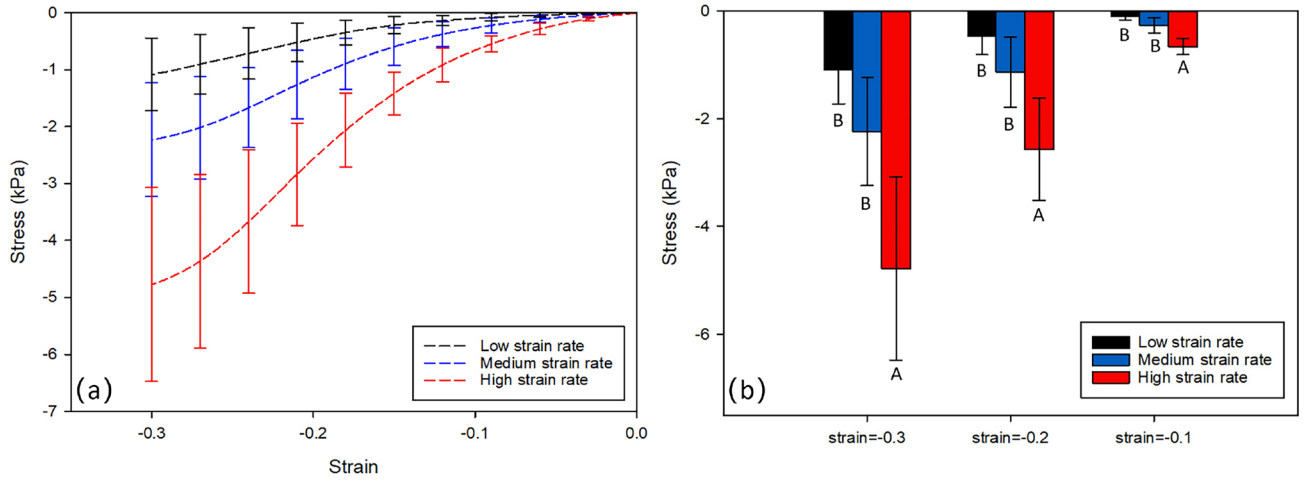

Fig. 4 (**a**) Mean compressive stress–strain response of brain tissue grouped by strain rate: low strain rate, medium strain rate and high strain rate. Error bars represent 95% confidence intervals of the stress. (**b**) Grouped vertical bars of stress levels (mean ± 95% confidence intervals) for brain tissue at 10, 20 and 30% strain increments for the three strain rate groups. In each strain rate group, stress levels not sharing a letter are considered significantly different (Tukey HSD)

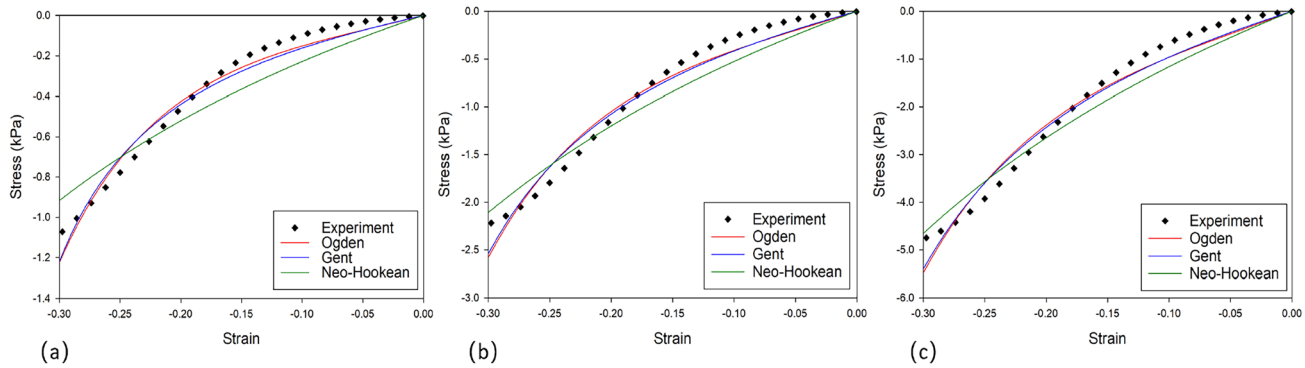

Fig. 5 Different hyperelastic strain-energy functions including Ogden, Gent and Neo-Hookean calibrated with mean experimental data of stress–strain response at (**a**) low, (**b**) medium and (**c**) fast strain rate group

Table 3 Constitutive parameters and corresponding coefficients of determination obtained by calibrating three hyperelastic constitutive models including Ogden, Gent and Neo-Hookean with mean time-independent elastic response at three strain rate groups

Large strain hyperelastic model parameter								
	Ogden			Gent			Neo-Hookean	
Strain rate	α	μ_0 (kPa)	R^2	J_m	μ_0 (kPa)	R^2	μ_0 (kPa)	R^2
0.01/s	13.65	0.51	0.98	0.71	0.46	0.97	0.68	0.91
1/s	11.17	1.38	0.97	0.95	1.21	0.97	1.57	0.93
10/s	10.04	3.23	0.96	1.13	2.79	0.97	3.47	0.95

immediate decrease after the compression platen was held and the stress increased with higher strain rate. It can be seen the most decay of stress occurred before 20 s, especially for a higher strain rate. For the reduced time constants in the Prony series, the starting values were assumed to be approximately equal to the average duration of loading in each strain rate group and a 3-term Prony series was applied. Table 4 summarizes the three pairs of viscoelastic parameters. Considering the lower relaxation percentage after 200 s at lower strain rate, the relaxation at higher strain rate

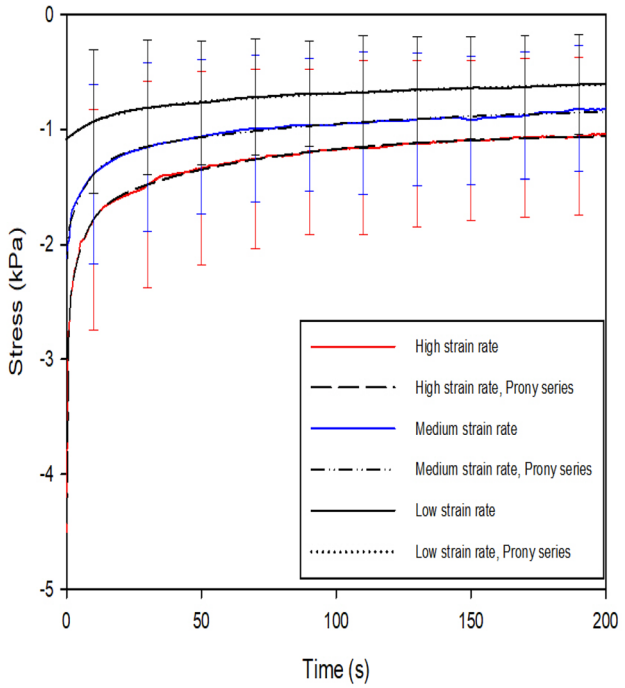

Fig. 6 Mean experimental data (full line) and Prony series model (dashed line) for compression relaxation at high, medium and low strain rates

appeared to respond faster with shorter time constants. The sensitivity of the time constants was observed with respect to the experimental data for the strain rate, especially for the longer time scale.

4 Discussion

The current experimental study provided novel insights into the compressive viscoelastic properties of pediatric brain tissue under linear and large strain. It has also provided analysis essential to establish and compare material constitutive models capable of predicting the corresponding mechanics of brain tissue. In agreement with previous studies on the adult porcine brain (Rashid et al. 2012; Thibault and Margulies 1998), the mechanical response of 4-month-old porcine brain tissue showed time and frequency dependent viscoelastic behavior. As compressive loading is the main cause for most blunt head trauma (Young et al. 2015; Bar-Kochba et al. 2016) and the impact loading sends stress waves through the skull resulting in brain damage such as contusion and hematomas (Hardman and Manoukian 2002), characterizing the time and frequency dependent viscoelastic response of pediatric brain tissue in compression is essential.

In comparison with a study on frequency-dependent viscoelastic properties of bovine brain tissue where the storage modulus increased across all frequencies (Li et al. 2021b), storage modulus in this study showed the limited capacity for additional stress-stiffening at higher frequencies. It indicated that the effect of lateral confinement in radial direction is more dominant with higher frequency, leading to the decrease in the elastic component of tissue modulus from axial direction. The mean complex modulus of brain tissue in this study was 13.02 kPa which is comparable to a study via oscillatory shear protocol on 1-year-old pig brain tissue with complex shear modulus of 12.49 kPa at 20 Hz (Thibault and Margulies 1998). However, a comparison of data obtained via loading protocols for shear and compression tests is limited because fundamentally the tests characterize different mechanical properties. With frequencies above 20 Hz, there was a gradual plateau in complex modulus indicating the balance occurred between the elastic and viscous response. The mean tan(delta) of tested brain samples increased significantly with frequency above 20 Hz, indicating the dominance of viscous response at higher frequencies. This may reflect injury adaptation as the brain tissue has been reported to be more susceptible to vibration at frequencies beyond 20 Hz (Laksari et al. 2018).

The large strain compressive response of 4-month-old porcine brain tissue at low, medium and high strain rates was compared with those in other studies of porcine brains at different ages under comparable strain level (Fig. 7) (Li et al. 2019; Tamura et al. 2007), which provides essential information on age dependence of pediatric brain material properties. Even though the experimental variability exists in the tests, the stress values are generally in the same level as the strain increases. The brain in this study showed limited capacity for further stress-stiffening beyond 0.2 strain, especially at higher strain rate. It may provide insights into why the brain tissue is easily injured at higher strain levels

Table 4 Viscoelastic parameters and coefficients of determination calibrated with the mean compression relaxation at three strain rates

Large strain viscoelastic model parameter							
	Coefficient			Relaxation time (s)			
Strain rate	g_1	g_2	g_3	τ_1	τ_2	τ_3	R^2
0.01/s	0.3	0.16	0.15	0.01	30.2	153.9	0.96
1/s	0.25	0.23	0.18	0.01	13.1	121.2	0.98
10/s	0.36	0.25	0.16	0.01	3.2	52.1	0.99

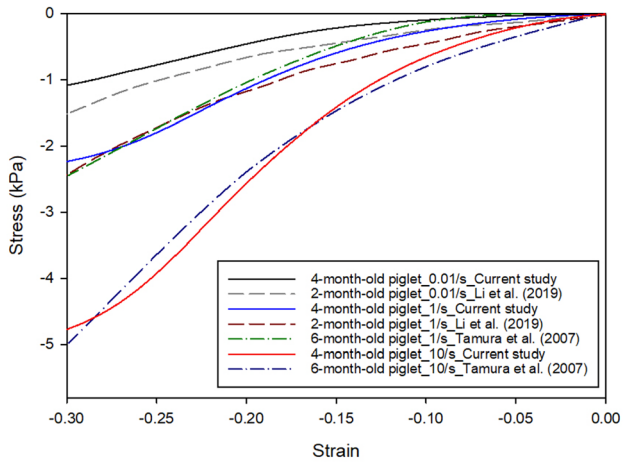

Fig. 7 Comparison of the compressive response of porcine brain tissue from different studies at three applied strain rates. The 4-month-old porcine brain tissue in this study showed limited capacity for further stress-stiffening beyond 0.2 strain, especially at a higher strain rate

and indicate that longitudinally compressed brain tissue was unable to accommodate higher strains, suggesting that the tissue may have mechanically failed or been irreversibly altered.

Although heterogeneity of brain tissue and variation between white and grey matter were previously studied (Elkin et al. 2011; Prange and Margulies 2002), our results provide a useful measure of the macroscopic mechanical response of pediatric brain tissue. Moreover, the average mechanical properties (mixed white and grey matter) of brain tissue have usually been analyzed in compression and indentation tests (Qian et al. 2018; Rashid et al. 2012). For brain injury, understanding the disparities between healthy and injured brain tissues is vital for advancing the comprehension of TBI mechanisms and developing effective diagnostic and therapeutic strategies. when brains subjected to traumatic forces, such as those experienced during TBI events, the mechanical behavior of brain tissues undergoes significant alterations. Therefore, there is a future opportunity to perform biomechanical testing of healthy and injured pediatric brain tissue samples to investigate the biomechanical changes induced by trauma.

In this study, linear viscoelastic models were applied to fit frequency-dependent values through Prony series representations following adaptation of the storage and loss moduli simultaneously. These models have the benefits of being easily applied in commercial software and more computationally cost effective. The mass density of brain tissue to be considered in numerical simulations is 1040 kg/m^3. The linear viscoelastic model was previously adopted to capture the small strain mechanical response of brain tissue with time-domain experimental data (Budday et al. 2017a, b; Qian et al. 2018). Although the model in the present study overestimated the dynamic storage modulus at frequencies above 20 Hz, not capable of describing the decreasing trend, all frequency-dependent viscoelastic response through linear viscoelastic models was approximated within the 95% confidence intervals of experimental data. Despite limited viscoelastic models in frequency domain compared with that in time domain, there is future opportunity for model development considering alternative boundary conditions. The viscoelastic parameters of brain tissue exhibited substantial differences between linear and large strain conditions. These variations were primarily due to the employment of distinct viscoelastic models and the acquisition of different experimental data.

A small amount of variability was encountered during sample preparation due to the soft nature of brain tissue leading to some deformation of specimens. Further, the samples were constrained to some extent in the radial direction presenting the limitations of measurement, especially at frequencies above 20 Hz. Although there was the decrease in the elastic component of tissue modulus with higher frequency, the trend of pediatric brain modulus was consistent with previous studies at tested frequencies below 20 Hz (Darvish and Crandall 2001; Li et al. 2021b).

5 Conclusion

To conclude, the viscoelastic behavior of pediatric porcine brain tissue was investigated in compression through DMA over a range of frequencies and at nonlinear deformation for three strain rates. The brain tissue is highly sensitive to the tested frequency and loading rate. Specifically, the complex modulus increased rapidly at lower frequencies with an average value of 13.02 kPa and stress increased at a higher strain rate. In this study, the constitutive properties of pediatric brain tissue were determined in terms of linear and large strain viscoelasticity, and the frequency and time dependent compressive behavior can be predicted satisfactorily through linear and quasi-linear viscoelastic models. The knowledge of the brain's viscoelastic properties is valuable to help improve the diagnosis of brain injury, to develop better smart head protection systems, and to establish complex head simulations.

Acknowledgements The authors would like to thank Lee Gauntlett from the Department of Mechanical Engineering, University of Birmingham for assistance in manufacturing of fixtures. This study was sponsored by the National Natural Science Foundation of China (Grant No. 12302417) and Shanghai Pujiang Program (23PJ1409200). The equipment used in this study was funded by Arthritis Research UK [H0671; now part of Versus Arthritis].

Author's contribution WL: Conceptualization, Methodology, Investigation, Writing - original draft, Writing - review & editing, Visualization, Project administration. DET: Resources, Writing review & editing, Supervision, Funding acquisition. DME: Methodology, Writing - review & editing, Supervision, Project administration.

Declarations

Conflict of interest The authors declare that they have no known competing financial interests or personal relationships that could have appeared to influence the work reported in this paper.

References

Araki T, Yokota H, Morita A (2017) Pediatric traumatic brain injury: characteristic features, diagnosis, and management. Neurol Med Chir (tokyo) 57:82–93. https://doi.org/10.2176/nmc.ra.2016-0191

Bar-Kochba E, Scimone MT, Estrada JB, Franck C (2016) Strain and rate-dependent neuronal injury in a 3D in vitro compression model of traumatic brain injury. Sci Rep 6:30550. https://doi.org/10.1038/srep30550

Barnes SC, Lawless BM, Shepherd DET, Espino DM, Bicknell GR, Bryan RT (2016) Viscoelastic properties of human bladder tumours. J Mech Behav Biomed Mater 61:250–257. https://doi.org/10.1016/j.jmbbm.2016.03.012

Bilston LE, Liu ZZ, Phan-Thien N (2001) Large strain behavior of brain tissue in shear: some experimental data and differential constitutive model. Biorheology 38:335–345

Budday S, Nay R, de Rooij R, Steinmann P, Wyrobek T, Ovaert TC, Kuhl E (2015) Mechanical properties of gray and white matter brain tissue by indentation. J Mech Behav Biomed Mater 46:318–330. https://doi.org/10.1016/j.jmbbm.2015.02.024

Budday S, Sommer G, Birkl C, Langkammer C, Haybaeck J, Kohnert J, Bauer M, Paulsen F, Steinmann P, Kuhl E, Holzapfel GA (2017a) Mechanical characterization of human brain tissue. Acta Biomater 48:319–340. https://doi.org/10.1016/j.actbio.2016.10.036

Budday S, Sommer G, Holzapfel GA, Steinmann P, Kuhl E (2017b) Viscoelastic parameter identification of human brain tissue. J Mech Behav Biomed Mater 74:463–476. https://doi.org/10.1016/j.jmbbm.2017.07.014

Burton H, Freij J, Espino DM (2017) Dynamic viscoelasticity and surface properties of porcine left anterior descending coronary arteries. Cardiovasc Eng Technol 8:41–56. https://doi.org/10.1007/s13239-016-0288-4

Chan RW, Titze IR (2003) Effect of postmortem changes and freezing on the viscoelastic properties of vocal fold tissues. Ann Biomed Eng 31:482–491. https://doi.org/10.1114/1.1561287

Chatelin S, Vappou J, Roth S, Raul JS, Willinger R (2012) Towards child versus adult brain mechanical properties. J Mech Behav Biomed Mater 6:166–173. https://doi.org/10.1016/j.jmbbm.2011.09.013

Chen Y, Qiu S, Wang C, Li X, Tang Y, Feng Y (2020) Measurement of viscoelastic properties of injured mouse brain after controlled cortical impact. Biophys Rep 6:137–145. https://doi.org/10.1007/s41048-020-00110-1

Cheng S, Bilston LE (2007) Unconfined compression of white matter. J Biomech 40:117–124. https://doi.org/10.1016/j.jbiomech.2005.11.004

Cheng S, Clarke EC, Bilston LE (2009) The effects of preconditioning strain on measured tissue properties. J Biomech 42:1360–1362. https://doi.org/10.1016/j.jbiomech.2009.03.023

Darvish KK, Crandall JR (2001) Nonlinear viscoelastic effects in oscillatory shear deformation of brain tissue. Med Eng Phys 23:633–645. https://doi.org/10.1016/S1350-4533(01)00101-1

Dickerson JWT, Dobbing J, McCance RA (1967) Prenatal and postnatal growth and development of the central nervous system of the pig. Proc R Soc Lond B Biol Sci 166:384–395. https://doi.org/10.1098/rspb.1967.0002

Elkin BS, Ilankova A, Morrison B (2011) Dynamic, regional mechanical properties of the porcine brain: indentation in the coronal plane. J Biomech Eng-Trans Asme. https://doi.org/10.1115/1.4004494

Fan H, Jin X, Hu J, Yanga KH (2014) Age dependent material properties of infant and adolescent porcine brain. Presented at the WSU 75th Anniversary Symposium Injury Biomechanics, Prevention, Diagnosis & Treatment, Detroit, MI, USA

Feng Y, Okamoto RJ, Namani R, Genin GM, Bayly PV (2013) Measurements of mechanical anisotropy in brain tissue and implications for transversely isotropic material models of white matter. J Mech Behav Biomed Mater 23:117–132. https://doi.org/10.1016/j.jmbbm.2013.04.007

Forte AE, Gentleman SM, Dini D (2017) On the characterization of the heterogeneous mechanical response of human brain tissue. Biomech Model Mechanobiol 16:907–920. https://doi.org/10.1007/s10237-016-0860-8

Franklyn M, Peiris S, Huber C, Yang KH (2007) Pediatric material properties: a review of human child and animal surrogates. Crit Rev Biomed Eng 35:197–342. https://doi.org/10.1615/critrevbiomedeng.v35.i3-4.20

Hardman JM, Manoukian A (2002) Pathology of head trauma. Neuroimaging Clin N Am 12:175–187. https://doi.org/10.1016/S1052-5149(02)00009-6

Hon KL, Huang S, Poon WS, Cheung HM, Ip P, Zee B (2019) Mortality and morbidity of severe traumatic brain injuries; a pediatric intensive care unit experience over 15 years. Bull Emerg Trauma 7:256–262. https://doi.org/10.29252/beat-070308

Laksari K, Kurt M, Babaee H, Kleiven S, Camarillo D (2018) Mechanistic insights into human brain impact dynamics through modal analysis. Phys Rev Lett 120:138101

Laksari K, Wu LC, Kurt M, Kuo C, Camarillo DC (2015) Resonance of human brain under head acceleration. J R Soc Interface. https://doi.org/10.1098/rsif.2015.0331

Li W, Shepherd DET, Espino DM (2021a) Investigation of the compressive viscoelastic properties of brain tissue under time and frequency dependent loading conditions. Ann Biomed Eng. https://doi.org/10.1007/s10439-021-02866-0

Li W, Shepherd DET, Espino DM (2021b) Dynamic mechanical characterization and viscoelastic modeling of bovine brain tissue. J Mech Behav Biomed Mater 114:104204. https://doi.org/10.1016/j.jmbbm.2020.104204

Li W, Shepherd DET, Espino DM (2020a) Frequency dependent viscoelastic properties of porcine brain tissue. J Mech Behav Biomed Mater 102:103460. https://doi.org/10.1016/j.jmbbm.2019.103460

Li Z, Ji C, Li D, Luo R, Wang G, Jiang J (2020b) A comprehensive study on the mechanical properties of different regions of 8-week-old pediatric porcine brain under tension, shear, and compression at various strain rates. J Biomech 98:109380. https://doi.org/10.1016/j.jbiomech.2019.109380

Li ZG, Yang HF, Wang GL, Han XQ, Zhang SP (2019) Compressive properties and constitutive modeling of different regions of 8-week-old pediatric porcine brain under large strain and wide strain rates. J Mech Behav Biomed Mater 89:122–131. https://doi.org/10.1016/j.jmbbm.2018.09.010

MacManus DB, Pierrat B, Murphy JG, Gilchrist MD (2017) A viscoelastic analysis of the P56 mouse brain under large-deformation dynamic indentation. Acta Biomater 48:309–318. https://doi.org/10.1016/j.actbio.2016.10.029

Mahmood H, Shepherd DET, Espino DM (2018) Surface damage of bovine articular cartilage-off-bone: the effect of variations in underlying substrate and frequency. BMC Musculoskelet Disord 19:384. https://doi.org/10.1186/s12891-018-2305-2

Meaney DF, Smith DH (2011) Biomechanics of concussion. Clin Sports Med 30:19–vii. https://doi.org/10.1016/j.csm.2010.08.009

Mendizabal A, Aguinaga I, Sánchez E (2015) Characterisation and modelling of brain tissue for surgical simulation. J Mech Behav Biomed Mater 45:1–10. https://doi.org/10.1016/j.jmbbm.2015.01.016

Miller K, Chinzei K (1997) Constitutive modelling of brain tissue: experiment and theory. J Biomech 30:1115–1121

Nguyen R, Fiest KM, McChesney J, Kwon C-S, Jette N, Frolkis AD, Atta C, Mah S, Dhaliwal H, Reid A, Pringsheim T, Dykeman J, Gallagher C (2016) The international incidence of traumatic brain injury: a systematic review and meta-analysis. Can J Neurol Sci J Can Sci Neurol 43:774–785. https://doi.org/10.1017/cjn.2016.290

Prange MT (2002) Biomechanics of traumatic brain injury in the infant. University of Pennsylvania

Prange MT, Margulies SS (2002) Regional, directional, and age-dependent properties of the brain undergoing large deformation. J Biomech Eng-Trans Asme 124:244–252. https://doi.org/10.1115/1.1449907

Pujalte GG, Dekker TM, Abadin AA, Jethwa TE (2020) Signs and symptoms of concussion. Concussion Manag. Prim. Care Evid. Based Answ. Cases Quest, pp 19–30

Qian L, Zhao H, Guo Y, Li Y, Zhou M, Yang L, Wang Z, Sun Y (2018) Influence of strain rate on indentation response of porcine brain. J Mech Behav Biomed Mater 82:210–217. https://doi.org/10.1016/j.jmbbm.2018.03.031

Qiu S, Jiang W, Alam MS, Chen S, Lai C, Wang T, Li X, Liu J, Gao M, Tang Y, Li X, Zeng J, Feng Y (2020) Viscoelastic characterization of injured brain tissue after controlled cortical impact (CCI) using a mouse model. J Neurosci Methods 330:108463. https://doi.org/10.1016/j.jneumeth.2019.108463

Rashid B, Destrade M, Gilchrist MD (2014) Mechanical characterization of brain tissue in tension at dynamic strain rates. J Mech Behav Biomed Mater 33:43–54. https://doi.org/10.1016/j.jmbbm.2012.07.015

Rashid B, Destrade M, Gilchrist MD (2012) Mechanical characterization of brain tissue in compression at dynamic strain rates. J Mech Behav Biomed Mater 10:23–38. https://doi.org/10.1016/j.jmbbm.2012.01.022

Roth S, Raul J-S, Willinger R (2010) Finite element modelling of paediatric head impact: global validation against experimental data. Comput Methods Prog Biomed 99:25–33. https://doi.org/10.1016/j.cmpb.2009.10.004

Sahoo D, Deck C, Willinger R (2014) Development and validation of an advanced anisotropic visco-hyperelastic human brain FE model. J Mech Behav Biomed Mater 33:24–42. https://doi.org/10.1016/j.jmbbm.2013.08.022

Szarko M, Muldrew K, Bertram JEA (2010) Freeze-thaw treatment effects on the dynamic mechanical properties of articular cartilage. Bmc Musculoskelet Disord. https://doi.org/10.1186/1471-2474-11-231

Takhounts EG, Crandall JR, Darvish K (2003) On the importance of nonlinearity of brain tissue under large deformations. Stapp Car Crash J 47:79–92

Tamura A, Hayashi S, Watanabe I, Nagayama K, Matsumoto T (2007) Mechanical characterization of brain tissue in high-rate compression. J Biomech Sci Eng 2:115–126. https://doi.org/10.1299/jbse.2.115

Thibault KL, Margulies SS (1998) Age-dependent material properties of the porcine cerebrum: effect on pediatric inertial head injury criteria. J Biomech 31:1119–1126. https://doi.org/10.1016/S0021-9290(98)00122-5

Velardi F, Fraternali F, Angelillo M (2006) Anisotropic constitutive equations and experimental tensile behavior of brain tissue. Biomech Model Mechanobiol 5:53–61. https://doi.org/10.1007/s10237-005-0007-9

Wilcox AG, Buchan KG, Espino DM (2014) Frequency and diameter dependent viscoelastic properties of mitral valve chordae tendineae. J Mech Behav Biomed Mater 30:186–195. https://doi.org/10.1016/j.jmbbm.2013.11.013

Yan J-G, Zhang L, Agresti M, LoGiudice J, Sanger JR, Matloub HS, Havlik R (2015) Neural systemic impairment from whole-body vibration. J Neurosci Res 93:736–744. https://doi.org/10.1002/jnr.23536

Young L, Rule GT, Bocchieri RT, Walilko TJ, Burns JM, Ling G (2015) When physics meets biology: low and high-velocity penetration, blunt impact, and blast injuries to the brain. Front Neurol 6:89. https://doi.org/10.3389/fneur.2015.00089

Zhao H, Yin Z, Li K, Liao Z, Xiang H, Zhu F (2016) Mechanical characterization of immature porcine brainstem in tension at dynamic strain rates. Med Sci Monit Basic Res 22:6–13. https://doi.org/10.12659/MSMBR.896368